INTERNATIONAL JOURNAL OF HYDROGEN ENERGY 35 (2010) 11768–11775

Available at www.sciencedirect.com

ScienceDirect

journal homepage: www.elsevier.com/locate/he

Photoelectrochemical hydrogen production from water/methanol decomposition using Ag/TiO_2 nanocomposite thin films

Naser Alenzi [a], Wei-Ssu Liao [b], Paul S. Cremer [b], Viviana Sanchez-Torres [c], Thomas K. Wood [c,d,e], Christine Ehlig-Economides [a], Zhengdong Cheng [c,*]

[a] Harold Vance Department of Petroleum Engineering, Texas A&M University, College Station, TX 77843, USA
[b] Department of Chemistry, Texas A&M University, College Station, TX 77843, USA
[c] Artie McFerrin Department of Chemical Engineering, Texas A&M University, College Station, TX 77843, USA
[d] Department of Biology, Texas A & M University, College Station, TX 77843-3258, USA
[e] Zachry Department of Civil and Environmental Engineering, Texas A & M University, College Station, TX 77843 3136, USA

ARTICLE INFO

Article history:
Received 18 April 2010
Received in revised form
2 August 2010
Accepted 5 August 2010
Available online 20 September 2010

Keywords:
Photoelectrochemical hydrogen production
Ag/TiO_2 nanocomposite thin film
Solar energy
Water-splitting
Nanotechnology

ABSTRACT

Though less frequently studied for solar-hydrogen production, films are more convenient to use than powders and can be easily recycled. Anatase TiO_2 films decorated with Ag nanoparticles are synthesized by a rapid, simple, and inexpensive method. They are used to cleave water to produce H_2 under UV light in the presence of methanol as a hole scavenger. A simple and sensitive method is established here to monitor the time course of hydrogen production for ultralow amounts of TiO_2. The average hydrogen production rate of Ag/TiO_2 anatase films is 147.9 ± 35.5 μmol/h/g. Without silver, it decreases dramatically to 4.65 ± 0.39 μmol/h/g for anatase TiO_2 films and to 0.46 ± 0.66 μmol/h/g for amorphous TiO_2 films fabricated at room temperature. Our method can be used as a high through-put screening process in search of high efficiency heterogeneous photocatalysts for solar-hydrogen production from water-splitting.

1. Introduction

Energy production and environmental challenges are paramount issues in the 21st century [1]. Limited fossil fuel resources and strict environmental regulations motivate the search for sustainable, efficient and environmentally friendly energy sources [2]. Hydrogen has great potential as a future energy carrier. It is the most abundant element on the earth. In fact, H_2 molecules have a higher energy content per weight than coal and gasoline [3]. Moreover, hydrogen can be used in fuel cells to generate electricity, or directly as a transportation fuel [4].

Hydrogen can be generated from hydrocarbons and water resources; however it does not exist in nature in its rich energy state. Currently, most hydrogen is produced from methane-steam reforming [5], which consumes energy and produces greenhouse gas emissions, mainly, carbon dioxide [4]. In contrast, a photoelectrochemical water-splitting process is a zero emission process and uses free solar energy [6–8].

* Corresponding author.
E-mail address: Cheng@chemail.tamu.edu (Z. Cheng).
0360-3199/$ – see front matter
doi:10.1016/j.ijhydene.2010.08.020

Extensive studies have been searching for the best material candidate for this process since it was discovered by Fujishama and Honda in 1972 [9]. The main criteria for these materials are low cost, environmentally friendly, high efficiency and stability. TiO_2 is a strong candidate due to its *high stability* in aqueous solutions and high photovoltaic and photocatalytic activity [10,11]. Nanotechnology, which manipulates materials at the nano or atomic scale, has a great potential for design and synthesis of multifunctional materials with desired and unique properties. It also can reduce the cost of materials manufacture. The purpose of this work is to pursue the possibility of using anatase Ag/TiO_2 nanocomposite films to generate hydrogen by water-splitting and improving their quantum efficiency.

To split water using photocatalytic materials and solar energy, there are three main obstacles need to be overcome: (1) narrowing of the band gap to harness visible light [12], (2) increasing the efficiency of charge separation, and (3) reducing the recombination reaction of O_2 and H_2 to form water [13]. Previous studies have focused heavily on these issues to find a strong candidate that matches all the criteria. The properties, size, geometry and compositions of materials are the keys to modify the material activity to improve hydrogen production [11]. Many tested semiconductors are either unstable in aqueous solution such as CdS, or possess too large a band gap such as SnO_2 [14].

Different semiconductor geometries have been extensively used in the harvesting of solar energy [15–17]. Nano-films are widely used to design photovoltaic solar cells [18]. However, to the best of our knowledge, only limited studies discussed nano-film TiO_2 for hydrogen production from the photoelectrochemical splitting of water. For example, Kitano, M. et al. in 2005 [19] reported that Pt-loaded visible light responsive TiO_2 thin films fabricated by the radio-frequency magnetron sputtering deposition (RF-MS) method decomposed water in the presence of methanol or silver nitrate solution under visible light irradiation.

The immobilization of the photocatalyst in the form of a thin film overcomes the drawbacks encountered with powder suspensions: (1) the difficulty of separating inactive catalysts, (2) the difficulty of applying them to continuous flow systems, and (3) the intendancy of the particle catalysts to aggregate. Novel methods to increase efficiency will enhance the appeal of photocatalyst thin films for applications [20].

In a photoelectrochemical process, the probability that separated charges will recombine highly depends on water solution additives and the metal loading of the semiconductor. After separation, electrons in the conduction band can be trapped by metal on the semiconductor's surface due to the difference in Fermi energies and work function. For water and methanol solutions, protons are generated via oxidation of water or methanol by holes. Then protons are reduced at the metal catalyst surface by electrons to produce hydrogen molecules. The following reactions occur during the process [21]:

$$h\upsilon \rightarrow e^- + \text{hole}^+,$$

$$4\text{hole}^+ + 2H_2O \rightarrow O_2\uparrow + 4H^+,$$

$$2H^+ + 2e^- \rightarrow H_2\uparrow.$$

The overall reaction is

$$4h\upsilon + 2H_2O \rightarrow O_2\uparrow + 2H_2\uparrow.$$

For water-splitting, the energy of the absorbed photon must be at least 1.23 eV [$E_i = \Delta G^\circ_{(water)}/2NA$ with $\Delta G^\circ_{(water)} = 237.141$ kJ/mol and NA = Avogadro's number = 6.022×10^{23}/mol] [21]. Methanol was added to water as strong oxidation agent (electron donor) in order to stop the oxygen gas that evolved when the water species adsorbed at photoanode (TiO_2 surface) get oxidized. Therefore, methanol is used here to efficiently separate the hole-charges, which leads to the reduction of hole-electron pair recombination process. This enables testing the activity of nanomaterials photocatalyst for water photoreduction reaction in a single photo-electrode system (photoreduction column) in simple, safe, flexible, accurate and inexpensive experimental set-up. However, in practical application, methanol will be replaced by photooxidation co-catalyst (e.g. nanocrystalline Fe_2O_3 ($E_g = 2.3$ eV)) which enable to use a two-column photo-electrodes (H-type photoelectrochemical cell or tandem cell system). In addition to its role as a hole scavenger, methanol may contribute to the generation of hydrogen via decomposition which enhances the overall hydrogen production rate. These side reactions also lead to the evolution of some carbon dioxide. The following reactions have been reported for methanol decomposition [21]:

$$MeOH \leftrightarrow H_2CO + H_2\uparrow,$$

$$H_2CO + H_2O \leftrightarrow H_2CO_2 + H_2\uparrow,$$

$$H_2CO_2 \leftrightarrow CO_2\uparrow + H_2\uparrow.$$

However, in this work we do not measure the CO_2 which may be evolved. An equal volume mixture of water and methanol solution is used based on previous studies [21].

The optimum band gap for solar-hydrogen production from water-splitting is between 1.5 and 2.0 eV to maximize the utilization of solar energy by harvesting the available visible light spectrum to split the water, in addition to overcome the thermodynamic losses [21]. The photons energy must match or be larger than the band gap energy of the semiconductor to be absorbed and excite the electrons. It is important to engineer the band gap of semiconductors to harness longer wavelength photons. To increase the hydrogen production from the photoelectrochemical water-splitting process, materials with appropriate properties (chemical, electronic, thermal, and optical, etc.) need to be tailored, fabricated, characterized and evaluated.

We present here Ag/TiO_2 nanocomposite films that are synthesized and evaluated as photocatalysts for hydrogen production. The fabrication method of Ag/TiO_2 films reported by Liao and Cremer [22,23] for biosensor applications [24] is modified to synthesize the anatase Ag/TiO_2 nanocomposite films. *Silver* nanoparticles are used here to effectively *separate* electron and hole pairs produced in the photoelectrochemical reactions. Prior to the silver deposition, the TiO_2 thin films were heated for 5 h at 500 °C to form the anatase crystal structure of TiO_2. We demonstrated herein a sensitive screening method for production of hydrogen from an ultralow amount of photocatalyst.

2. Experimental

2.1. *Materials and synthesis of Ag/TiO_2 nanocomposite films*

As noted above, Ag/TiO_2 films were synthesized by following the procedure developed by Liao and Cremer [22,23] with a modification to form anatase TiO_2. The precursor solution for TiO_2 consisted of 1 g of titanium (IV) isopropoxide (Sigma–Aldrich), 0.15 g of HCl (Fisher Scientific), and 8.0 g of isopropyl alcohol (Sigma–Aldrich). Polished Pyrex 7740 wafers (25.4 mm^2, 0.5 mm thick) were purchased from Precision Glass and Optics (Santa Ana, CA). The Pyrex wafers were cleaned in piranha solution for 45 min (1:3 ratio of 30% H_2O_2 and H_2SO_4), and rinsed extensively with purified water (18.2 $M\Omega/cm^2$, NANO pure Ultrapure Water System, Barnstead, Dubuque, IA), dried with nitrogen, and heated at 500 °C for 5 h.

The precursor solution was prepared by first adding titanium (IV) isopropoxide followed by the acid. A TiO_2 film was made by depositing approximately 150 μL of the solution onto the Pyrex wafer dropwise. After waiting for 5–10 min for the precursor to dry, the sample was heated to 500 °C for 5 h to form the anatase crystal structure of TiO_2, which is known to be more photocatalytically active and more thermally stable than the rutile and brookite crystal structures of TiO_2 [25]. Silver nitrate (Sigma–Aldrich) is used for the reduction of silver from a 0.1 M aqueous silver nitrate solution; it is performed with a standard 420 W Hg Arc lamp (Newport, Model 97435-1000-1, Oriel Instruments, CA, USA) as the UV light source. The aqueous silver nitrate solution was dropped inside a polydimethylsiloxane (PDMS) well. The light illuminated the TiO_2 through the Pyrex side of the sample. The Pyrex sample is transparent in the near UV range, which is the critical wavelength region for reducing silver ions from solution. Fig. 1 illustrates the fabrication procedures.

2.2. *Nanocomposite film characterizations*

After synthesis, the Ag/TiO_2 nanocomposite films were characterized using Scanning Electron Microscopy (SEM) (Fig. 2). The SEM images were taken using JEOL JSM-6400. The Surface element analysis was obtained using Energy dispersive X-ray spectroscopy (EDS) as shown in Table 1. The EDS results were obtained using JEOL JSM-6400. The peak positions and chemical compositions were obtained using X-ray photoelectron spectrometer (XPS) as shown in Fig. 3 and Table 2. The XPS results were obtained using a Kratos Axis Ultra Imaging X-ray photoelectron spectrometer. Fig. 4(a–d) showed the X-ray diffraction (XRD) patterns of the Ag/TiO_2 film and the TiO_2 film with and without annealing. The powder X-ray diffraction data was collected using a Bruker D8 Advance powder diffractometer (CuKα; λ = 1.5418 Å) fitted with LynxEye detector. Fig. 5 showed the UV–visible spectra of TiO_2 film

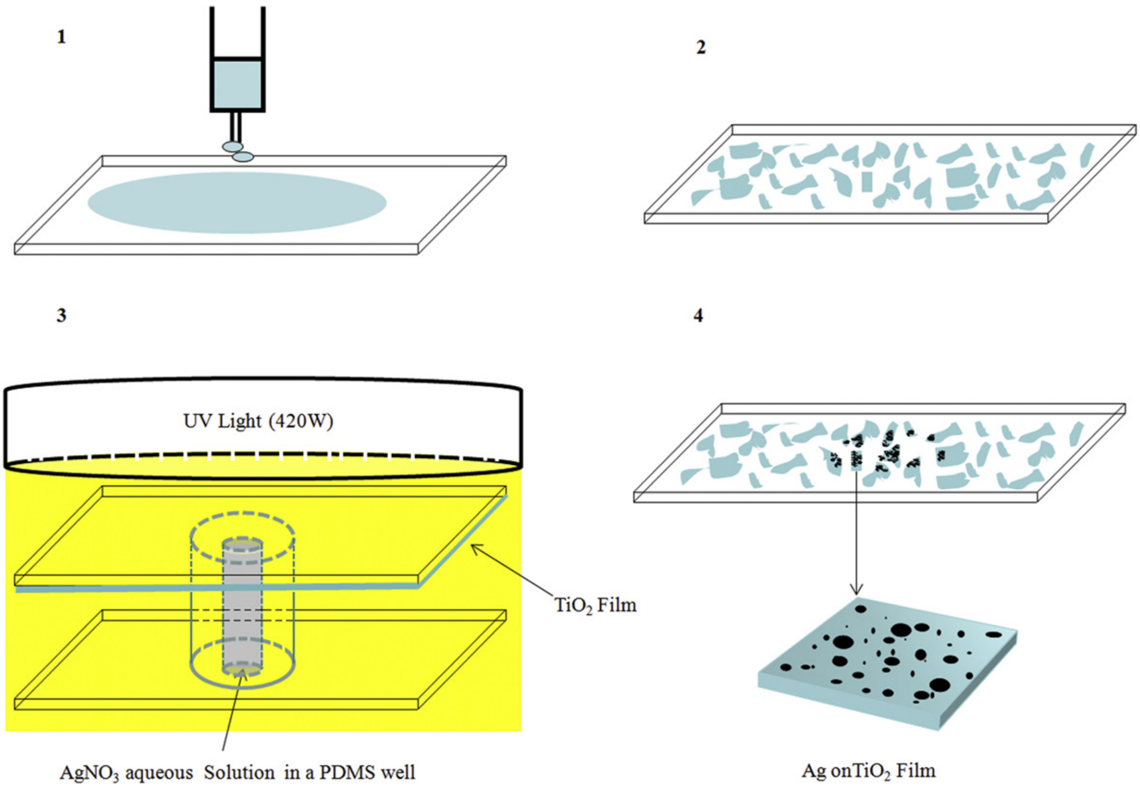

Fig. 1 – Schematic diagram for the fabrication procedure of Ag/TiO_2 nanocomposite films. (1) A TiO_2 precursor is dropped onto a 2.5 cm × 2.5 cm planar Pyrex substrate. (2) The thin layer is dried and heated to 500 °C for 5 h to form islands of anatase TiO_2 films. (3) A $AgNO_3$ aqueous solution is dropped into a PDMS well, and silver is reduced by a photoelectron using UV radiation (420 W and Ag deposition time is 5 min). (4) The Ag/TiO_2 thin film is washed with water and ethanol and dried with nitrogen.

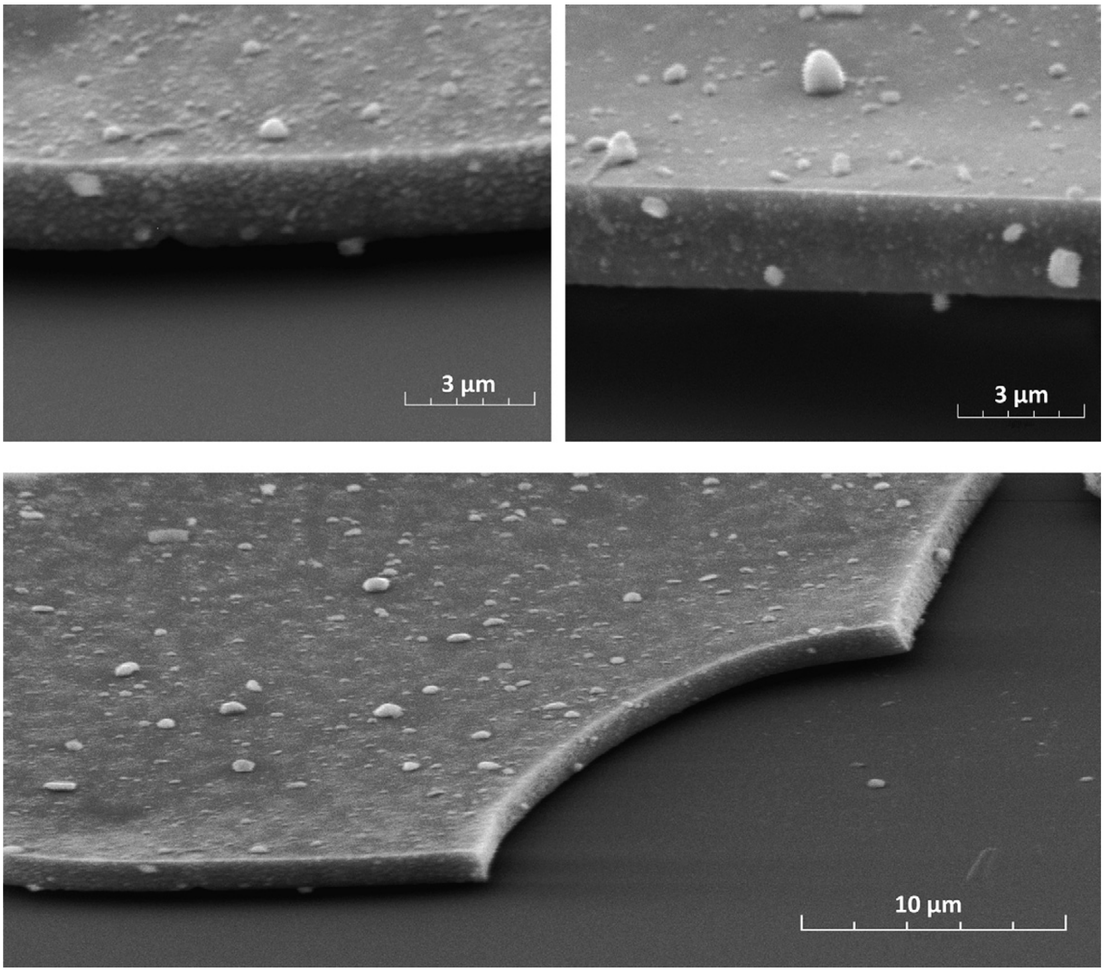

Fig. 2 – SEM micrographs of Ag/TiO_2 nanocomposite films. The averaged film thickness is about 2.0 ± 0.2 µm. The size of the Ag nanoparticles deposited on the TiO_2 films is not uniform. The averaged size of Ag nanoparticles is around 200 ± 50 nm.

(anatase). The UV–vis–NIR spectrophotometer was measured using a Hitachi U4100 with an integrating sphere.

2.3. *Photoelectrochemical hydrogen production*

The experiments were carried out in a Pyrex flask (250 ml, transparent in the near UV range). A 10 ml 1:1 volume mixture of water and methanol was added. The photocatalyst (Ag/TiO_2 thin-film sample) was inserted into the flask carefully, and immersed just under the water/methanol solution surface. The 250 ml Pyrex flask was well sealed by a silicon septum.

Table 1 – Surface element analysis using EDS.

Glass surface		Particle surface		Surface of TiO_2 film	
Element	Wt%	Element	Wt%	Element	Wt%
Al	5.36	Ti	38.64	Ti	83.01
Si	92.79	Pd	0.00	Pd	0.50
K	1.86	Ag	57.59	Ag	12.96
		Au	3.77	Au	3.54
Total	100	Total	100	Total	100

Prior to the reaction, the solution was purged with nitrogen (from 30 to 60 min) to remove air from the flask as well as the air and oxygen species dissolved in the solution. Hydrogen was detected before the reaction (usually it is less than

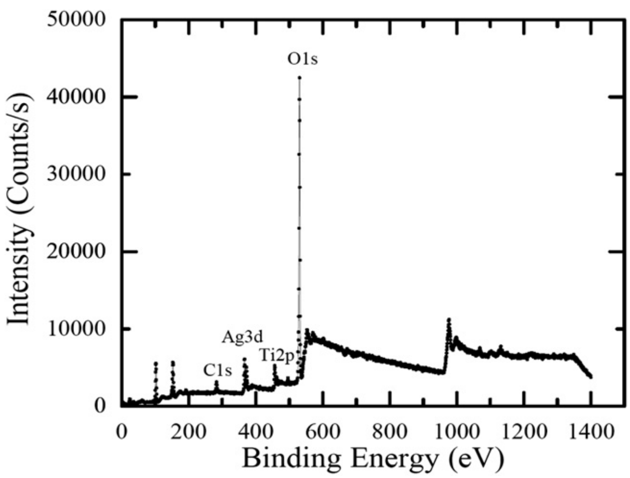

Fig. 3 – XPS of a Ag/TiO_2 nanocomposite film shows intensity versus binding energy for all components.

Table 2 – The peaks, atomic concentration and mass concentration from XPS analysis.

Peak	Position BE (eV)	FWHM (eV)	Raw Area (CPS)	RSF	Atomic mass	Atomic Conc. %	Mass Conc. %
O1s	530.55	1.542	22002.8	0.78	15.999	94.62	79.76
Ti 2p	456.55	1.181	1873.8	2.001	47.878	3.26	8.23
Ag 3d	366.25	1.282	3484.2	5.987	107.878	2.11	12.01

3.00 ± 0.25 μmol) and all data are reported with this background subtracted. UV light (Long Wave Ultraviolet lamp, Model B-100AP, UVP, CA, USA) illuminated the reaction cell. The straight distance between the UV source and the photocatalyst sample was 16 ± 1.0 cm; vertical and horizontal measurements were carried out using a smart UV intensity meter and it was found that the maximum power intensity possible hitting the photocatalyst sample was 10 m W/cm^2. The reaction cell and the lamp were fully covered with alumina foil to avoid light leakage for safety considerations. Hydrogen generated in the head space of the flask was measured using a 50 μL aliquot by gas chromatography (GC) using a 6890 N gas chromatograph (Agilent Technologies, Glastonbury, CT) equipped with a 80–100 mesh Porapak Q column (Suppelco, Bellefonte, PA) and a thermal conductivity detector. The injector temperature was 100 °C and detector temperature was 200 °C. The pressure of nitrogen as carrier gas was 15 psi and the flow rate was 21 ml/min. The temperature of the column was 70 °C. The retention time for hydrogen was 0.4 min and the sensitivity was about 0.1 μmol for the above conditions. Retention times were determined by comparisons to neat standards as well as by co-elution with standards [26,27].

3. Results and discussion

The SEM micrographs revealed that the averaged film thickness was about 2.0 ± 0.2 μm and the silver nanoparticles were 200 ± 50 nm. The SEM images showed that the TiO_2 layer broke down to islands during annealing to 500 °C. The images also showed that the size of silver nanoparticles deposited on TiO_2 films was not uniform by the photodeposition technique used here.

The XPS presented the surface element analysis including the atomic concentration and mass concentration. The peaks are consistent with literature data for the binding energy of O1s, Ti2p and Ag3d [28].

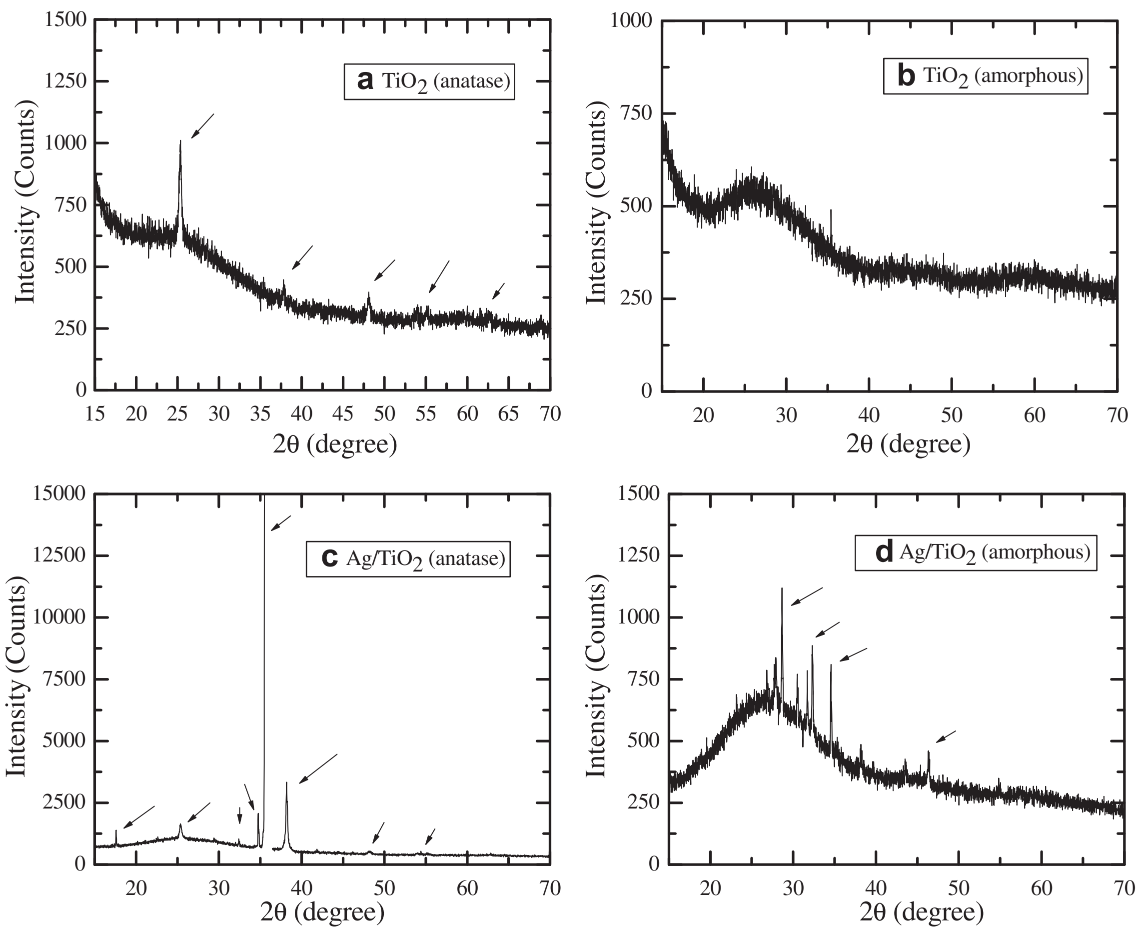

Fig. 4 – XRD patterns of (a) TiO_2 (anatase). (b) TiO_2 (amorphous). (c) Ag/TiO_2 (anatase). (d) Ag/TiO_2 (amorphous).

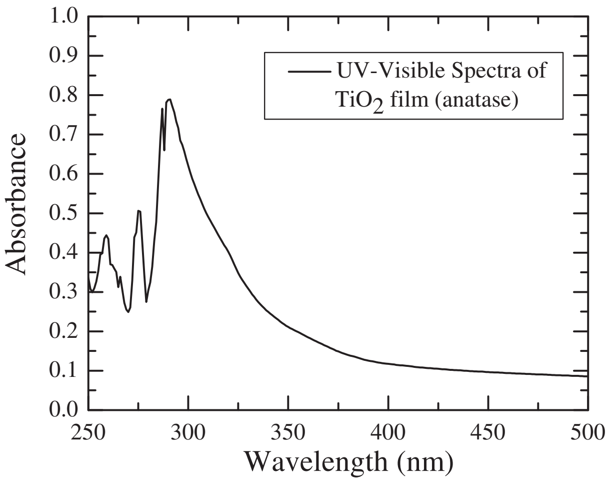

Fig. 5 – UV–visible spectra of anatase TiO_2 film (after annealing at 500 °C for 5 h).

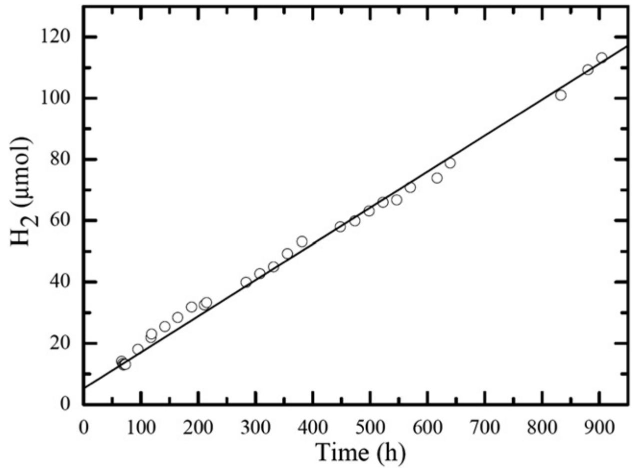

Fig. 6 – Time course of hydrogen production using anatase Ag/TiO_2 nanocomposite films. The slope gives the production rate of this run as 188.7 ± 0.39 μmol/h/g. The weight of photocatalyst used in this run was estimated to be 0.58 mg. The stability of the hydrogen production rate using Ag/TiO_2 nanocomposite films exceeded one month in experimental duration.

The EDS results presented in Table 1 showed the weight percentage of glass surface, particle surface, and the surface of TiO_2 film. The Au and Pd were deposited on the film surface in order to do the SEM analysis.

To confirm how the anatase Ag/TiO_2 film has a substantial impact on film reactivity and also to compare the amorphous TiO_2 with anatase crystal structure TiO_2, X-ray diffraction (XRD) patterns characterization shown in Fig. 4(a–d) revealed the crystal structure of anatase TiO_2. The XRD patterns of amorphous TiO_2 showed no crystallites existed. For anatase Ag/TiO_2, it showed the diffraction peaks of crystallites silver, anatase TiO_2 nanocrystals and crystals of some impurities due to the silver present on the surface of TiO_2. For amorphous Ag/TiO_2, it showed the diffraction peaks of crystallites silver and crystal peaks from some impurities due to the silver present on the surface of TiO_2 as well, which may react with other elements on the air such as oxygen.

To demonstrate the band gap of anatase TiO_2 film, UV–visible spectra presented in Fig. 5 showed that the absorbance wavelength of anatase TiO_2 film in the range of 290–320 nm. The higher absorbance wavelength of anatase TiO_2 means lower in band gap according to Planck–Einstein equation ($E = hc/\lambda$).

Fig. 6 shows the hydrogen evolution for one of the three runs conducted using the Ag/TiO_2 films. The averaged hydrogen production rate was found to be 147.9 ± 35.5 μmol/h/g. The standard deviation for the three experiments was used to report the error. These variations might be attributed to films deactivation by air oxidation when exposed to the atmosphere during sample storage, or due to weight estimation errors. The Ag/TiO_2 nanocomposite films showed a high stability for the hydrogen production rate which exceeded one month.

The fabrication of Ag/TiO_2 nanocomposite films [22,23] has been modified to form the anatase crystal structure of TiO_2 since it is known that this structure is more photocatalytically active. Previously, Jeon et al. [29] tested Cu/TiO_2 powdered photocatalysts, 20 g, under 36 W/m^2 UV, revealed a hydrogen production of 648.52 μmol/h. For comparison, the data will be scaled to a light power of 100 W/m^2 and a unit sample weight of 1 g, which gives 90.07 μmol/h/g. Clearly, the hydrogen production rate from their powdered Cu/TiO_2 is less than the hydrogen production rate of the Ag/TiO_2 nanocomposite film presented in this work. This may be attributed to the tendency of the powder to aggregate, which reduces the surface area exposed to the electrolyte solution and the overall reactivity. Also the metal–TiO_2 contact should be different due to the

Table 3 – Comparison of the hydrogen production rate from water/methanol decomposition under UV light, scaling to 100 W/m^2 power intensity and 1 g photocatalyst weight.

No.	Photocatalyst	H_2 production (μmol/h/g)	Solution ratio (1:1, v/v)	Nanostructure	Reference	Parameters affect reactivity
1	Cu/TiO_2 (500 °C)	90.07	water/MeOH	Powder	[29]	Geometry
2	Ag/TiO_2 (anatase)	147.9 ± 35.5	water/MeOH	Thin Film	This work	Metal
3	TiO_2 (anatase)	4.65 ± 0.39	water/MeOH	Thin Film	This work	Crystal structure
4	TiO_2 (amorphous)	0.46 ± 0.66	water/MeOH	Thin Film	This work	–

Note: Between 1 & 2, the metal particle size and amount are also different.

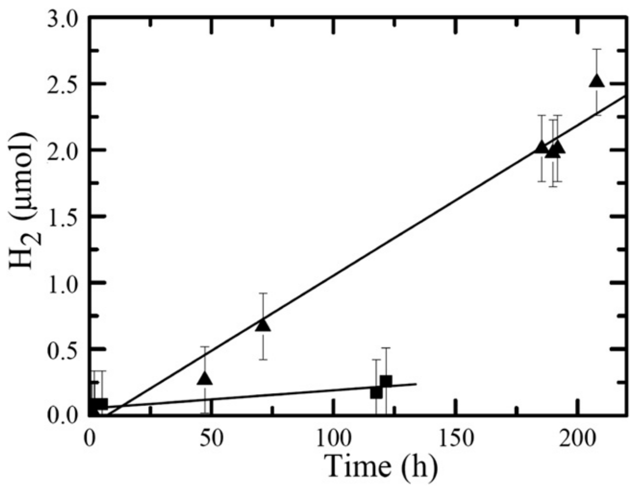

Fig. 7 – The time course of hydrogen production from TiO_2 films without silver deposition. The hydrogen evolution was extremely low, 0.46 ± 0.66 μmol/h/g, for the non annealed (room temperature, amorphous TiO_2) sample (squares), while the annealed (at 500 °C for 5 h, anatase crystal structure TiO_2) sample (triangles) showed a slight improved hydrogen production rate of 4.65 ± 0.39 μmol/h/g.

preparation procedures. The small difference in the work function of Ag and Cu may also influence the electron transport from the TiO_2 conduction band to the metal surface. It is possible that the size of the metal particles could create defects in the crystal structure and change the electronic confinement in TiO_2. Beside higher activity, our film can be easily recycled. Table 3 illustrated the comparison of results between this work and Jeon et al. [29] to investigate the effect of TiO_2 geometry, metal, and TiO_2 crystal structure on hydrogen production rate.

As a control, the performance of the anatase TiO_2 thin film was probed without silver deposition. As shown in Fig. 7, the hydrogen production rate for an anatase TiO_2 nanocomposite film without Ag is about 4.65 ± 0.39 μmol/h/g, which represents an enormous reduction in the hydrogen production rate. To investigate possible crystal structure effects, a Ag/TiO_2 thin film was synthesized without the annealing step (at 500 °C for 5 h). This film exhibited a hydrogen production rate of 0.46 ± 0.66 μmol/h/g. It is clear that the anatase crystal structure (produced at 500 °C for 5 h) of the TiO_2 thin film has a substantial impact on the film's activity. This can be attributed to changes in the electronic structure, electron confinement, and electron excitation between the crystalline and non-crystalline materials. Therefore, the Ag/TiO_2 nanocomposite film structure can be thought to facilitate the transportation of electrons from TiO_2 to the Ag surface which in turn enhances the hydrogen production rate.

Due to its simplicity, low cost and high sensitivity to monitor the time course and hydrogen production rate, our method can be implemented as a high through-put screening process to search for high efficiency ultrathin films or nanostructures for Photocatalytic solar-hydrogen production via the splitting of water. The method may also be very helpful to investigate the influence of many parameters on hydrogen production rate such as new materials, nanocomposites, additives, water purity, light intensity inside the laboratory and outside under direct sunlight. It will contribute to a better understanding of material function and photoelectrochemical reaction mechanism.

4. Conclusions

The feasibility of generating hydrogen photoelectrochemically from water/methanol decomposition using Ag/TiO_2 nanocomposite films has been demonstrated. The overall activity of hydrogen production was 147.9 ± 35.5 μmol/h/g. In addition, the Ag/TiO_2 nanocomposite films showed high stability for hydrogen production for more than one month. Thin-film photocatalysts have an advantage in that they can be regenerated or reuse unlike the powdered catalysts. Previous fabrication of Ag/TiO_2 nanocomposite film [22,23] was modified to form the anatase crystal structure of TiO_2. This was observed to enchance the photocatalytic properties of these materials.

Our test methodology of detecting hydrogen production from an ultralow amount of photocatalyst can be used as a high through-put screening process to search for high efficiency photocatalysts for hydrogen production by photoelectrochemical water-splitting using solar energy.

Acknowledgments

This work was supported by startup funds from the Texas Engineering Experiment Station (TEES), Texas A&M University, and by the National Science Foundation (CBET-0753702). PSC and WSL thank the VPR Energy Resources Program for further support. We would also like to thank the Kuwait Institute for Scientific Research as the sponsor for Naser Alenzi. We thank Dr. Amanda Young for help with UV–visible spectra. We thank Dr. Nattamai Bhuvanesh for help with XRD. We thank Dr. Gang Liang for help with XPS. Finally, we thank Mr. Inho Lee for help with the EDS and SEM images.

REFERENCES

[1] Hassmann K, Kuhne HM. Primary energy sources for hydrogen production. Int J Hydrogen Energy 1993;18:635–40.

[2] Dunn S. Hydrogen futures: toward a sustainable energy system. Int J Hydrogen Energy 2002;27:235–64.

[3] Wilhelm E, Fowler M. A technical and economic review of solar hydrogen production technologies. Bull Sci Technol Soc 2006;26:278–87.

[4] Dougherty W, Kartha S, Rajan C, Lazarus M, Bailie A, Runkle B, et al. Greenhouse gas reduction benefits and costs of a large-scale transition to hydrogen in the USA. Energy Policy 2009;37:56–67.

[5] Kikuchi E, Nemoto Y, Kajiwara M, Uemiya S, Kojima T. Steam reforming of methane in membrane reactors: comparison of electroless-plating and CVD membranes and catalyst packing modes. Catal Today 2000;56:75–81.

[6] Currao A. Photoelectrochemical water splitting. CHIMIA Int J Chem 2007;61:815–9.

[7] Nowotny J, Bak T, Nowotny MK, Sheppard LR. Titanium dioxide for solar-hydrogen. I. Functional properties. Int J Hydrogen Energy 2007;32:2609–29.
[8] Nowotny J, Bak T, Nowotny MK, Sheppard LR. Titanium dioxide for solar-hydrogen. II. Defect chemistry. Int J Hydrogen Energy 2007;32:2630–43.
[9] Fujishima A, Honda K. Electrochemical photolysis of water at a semiconductor electrode. Nature 1972;238:37–8.
[10] Murphy AB, Barnes PRF, Randeniya LK, Plumb IC, Grey IE, Horne MD, et al. Efficiency of solar water splitting using semiconductor electrodes. Int J Hydrogen Energy 2006;31:1999–2017.
[11] Ni M, Leung MKH, Leung DYC, Sumathy K. A review and recent developments in photocatalytic water-splitting using TiO_2 for hydrogen production. Renew Sustain Energ Rev 2007;11:401–25.
[12] Zou Z, Ye J, Sayama K, Arakawa H. Direct splitting of water under visible light irradiation with an oxide semiconductor photocatalyst. Nature 2001;414:625–7.
[13] Osterloh FE. Inorganic materials as catalysts for photochemical splitting of water. Chem Mater 2008;20:35–54.
[14] Matsuoka M, Kitano M, Takeuchi M, Tsujimaru K, Anpo M, Thomas JM. Photocatalysis for new energy production – recent advances in photocatalytic water splitting reactions for hydrogen production. Catal Today 2007;122:51–61.
[15] Steinfeld A. Solar hydrogen production via a two-step water-splitting thermochemical cycle based on Zn/ZnO redox reactions. Int J Hydrogen Energy 2002;27:611–9.
[16] Licht S, Wang B, Mukerji S, Soga T, Umeno M, Tributsch H. Over 18% solar energy conversion to generation of hydrogen fuel; theory and experiment for efficient solar water splitting. Int J Hydrogen Energy 2001;26:653–9. Reprinted from J Phys Chem B 2000;104:8920–8924.
[17] Kudo A. Development of photocatalyst materials for water splitting. Int J Hydrogen Energy 2006;31:197–202.
[18] Shah A, Torres P, Tscharner R, Wyrsch N, Keppner H. Photovoltaic technology: the case for thin-film solar cells. Science 1999;285:692–8.
[19] Kitano M, Takeuchi M, Matsuoka M, Thomas JM, Anpo M. Preparation of visible light-responsive TiO_2 thin film photocatalysts by an RF magnetron sputtering deposition method and their photocatalytic reactivity. Chem Lett 2005;34:616–7.
[20] Arabatzis IM, Stergiopoulos T, Bernard MC, Labou D, Neophytides SG, Falaras P. Silver-modified titanium dioxide thin films for efficient photodegradation of methyl orange. Appl Catal B Environ 2003;42:187–201.
[21] Choi H-J, Kang M. Hydrogen production from methanol/water decomposition in a liquid photosystem using the anatase structure of Cu loaded TiO_2. Int J Hydrogen Energy 2007;32:3841–8.
[22] Liao WS, Yang T, Castellana ET, Kataoka S, Cremer PS. A rapid prototyping approach to Ag nanoparticle fabrication in the 10–100 nm range. Adv Mater (Weinheim Ger) 2006;18:2240–3.
[23] Castellana ET, Kataoka S, Albertorio F, Cremer PS. Direct writing of metal nanoparticle films inside sealed microfluidic channels. Anal Chem 2006;78:107–12.
[24] Liao WS, Chen X, Yang T, Castellana ET, Chen J, Cremer PS. Benchtop chemistry for the rapid prototyping of label-free biosensors: transmission localized surface plasmon resonance platforms. Biointerphases 2009;4:80–5.
[25] Kato K, Tsuzuki A, Taoda H, Torii Y, Kato T, Butsugan Y. Crystal structures of TiO_2 thin coatings prepared from the alkoxide solution via the dip-coating technique affecting the photocatalytic decomposition of aqueous acetic acid. J Mater Sci 1994;29:5911–5.
[26] Maeda T, Vardar G, Self WT, Wood TK. Inhibition of hydrogen uptake in *Escherichia coli* by expressing the hydrogenase from the cyanobacterium *Synechocystis* sp. PCC 6803. BMC Biotechnol 2007;7:25.
[27] Maeda T, Sanchez-Torres V, Wood TK. Enhanced hydrogen production from glucose by metabolically engineered *Escherichia coli*. Appl Microbiol Biotechnol 2007;77:879–90.
[28] Ge L, Xu MX, Fang HB. Photo-catalytic degradation of methyl orange and formaldehyde by Ag/$InVO_4$–TiO_2 thin films under visible-light irradiation. J Mol Catal A-Chemical 2006;258:68–76.
[29] Jeon MK, Park JW, Kang M. Hydrogen production from methanol/water decomposition in a liquid photosystem using the anatase and rutile forms of Cu–TiO_2. J Ind Eng Chem 2007;13:84–91.